A Three-phase MVAC to Multi-port LVDC Converter with High Frequency Isolation for Fast DC Charging Station for EVs

Harisyam P V
Electrical Engineering Dept.
Indian Institute of Science
Bengaluru, India
harisyamv@iisc.ac.in

Saichand Kasicheyanula
Delta Electronics, India
Bengaluru, India
Saichand.Kasicheyanu
@deltaww.com

Shashidhar Mathapati
Delta Electronics, India
Bengaluru, India
shashidhar.mathapati
@deltaww.com

Kaushik Basu
Electrical Engineering Dept.
Indian Institute of Science
Bengaluru, India
kbasu@iisc.ac.in

2023 IEEE Energy Conversion Congress and Exposition (ECCE) | 979-8-3503-1644-5/23/$31.00 ©2023 IEEE | DOI: 10.1109/ECCE53617.2023.10362814

***Abstract*—A DC fast charging station for electric vehicles (EV) comprising multiple high-power EV chargers consumes a significant amount of power in the range of 1MW from the AC side. Today a 50Hz transformer is used to step down Medium Voltage (MV) AC (11kV) to Low Voltage (LV) AC (400V), after which several AC-DC converters followed by isolated DC-DC converters are used to create isolated DC ports for charging EV batteries and to integrate local storage and solar PV. This solution has a large and expensive 50Hz transformer and multiple conversion stages, resulting in poor efficiency, power density, and high cost. This paper presents a novel MVAC to multi-port LVDC converter with high-frequency isolation. The proposed modulation strategy ensures bidirectional power flow at all ports and equal sharing of active power in all three MVAC phases, while unequal power is transferred between different LVDC ports. Power factor correction or reactive power support is also possible for the proposed configuration. The operation is verified using simulation tools along with experimental verification.**

***Index Terms*—MVAC, Multiport DC, Dual Active Bridge, Fast charging, Electric Vehicle**

I. Introduction

With the penetration of renewable and energy storage devices, there is a significant increase in grid-connected LVDC systems. In an electric bus charging station consisting of multiple EV chargers, the power requirements of the charging station could well exceed 1 MVA [1]. The current state-of-the-art AC-connected system uses a line frequency transformer (LFT) to step down MVAC to LVAC, and then there are individual AC-DC stages followed by an isolated DC-DC stages per individual DC port, Fig. 1. The number of power stages involved in an AC-coupled system is higher when the power transfer happens from one DC port to another port. This is relevant when power from renewable is used for charging, vehicle to vehicle (V2V) charging, and while consuming stored energy in battery bank. The line frequency transformer involved in this solution is also quite bulky, expensive and reduces the overall system's efficiency and power density.

This work was supported in part by the Department of Science and Technology, Government of India under the project titled "Medium Voltage Grid Integration of Utility-Scale Renewable " through the Core Research Grant scheme.

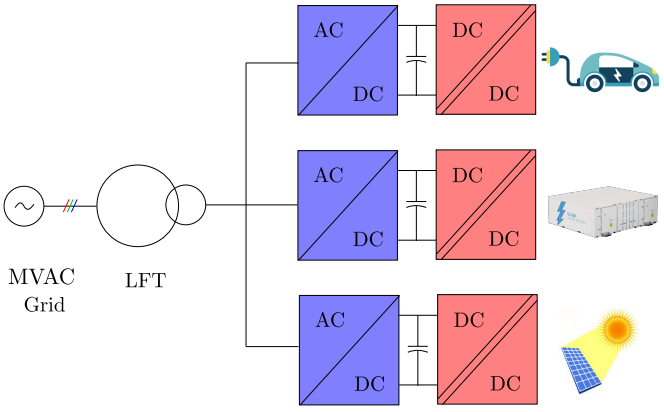

Fig. 1. State of the art AC connected system for commercial products

In this context, high-frequency link MVAC to LVDC conversion is a way to eliminate heavy line frequency transformers, which require a large amount of iron and copper. Power converters for generation of multiple LVDC ports from MVAC can be broadly classified based on the intermediate stage utilized viz., (a) using an intermediate MVDC bus [2] and (b) using Cascaded H-Bridge (CHB) based input series output parallel (ISOP) configuration [3]. In the first category (Fig. 2), a two-stage configuration involving a non-isolated MVAC-MVDC converter stage followed by an MVDC-isolated LVDC converter stage is utilized. In this method, MVDC from MVAC can be generated either using MMC [4] or using traditional AC-DC converters based on MV semiconductor devices [2]. These MV devices are commercially not available and result in EMI issues due to high dv/dt. MMC-based topologies needs to maintain a MVDC bus of twice the peak of line to neutral voltage. They require higher insulation, voltage balancing circuit for the MVDC bus, and has higher semiconductor switch count [4], [5]. MV high-frequency AC applied to the high frequency transformer in MVDC to LVDC converter makes magnetics design challenging.

The second category in MVAC-LVDC converters utilizes

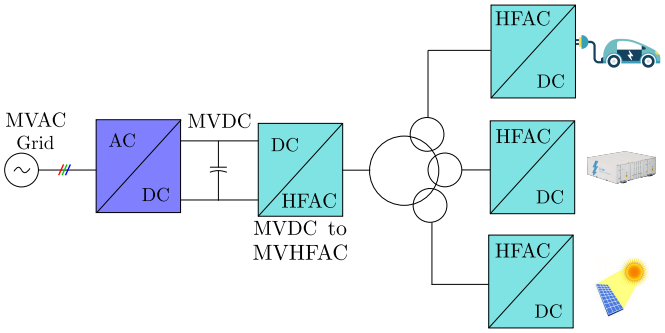

Fig. 2. MVAC to LVDC solution with intermediate MVDC bus

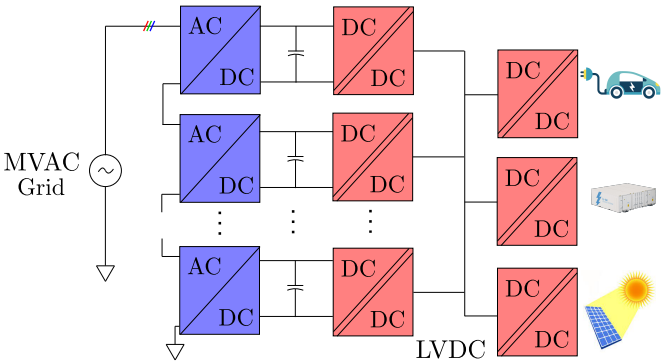

Fig. 3. Input series output parallel (ISOP) multi level configuration

CHB-based Input Series Output Parallel (ISOP) configuration, Fig. 3. In this configuration, multiple non-isolated LVDC ports of the CHB converter are combined through isolated DC-DC conversion stages to generate a single isolated LVDC bus. Multiple LVDC ports are generated from this LVDC bus using the next stage of isolated DC-DC converters [6]. This configuration is economical due to lower insulation requirements (corresponding to peak phase voltage) compared to intermediate MVDC bus configuration. However, multiple isolated DC-DC conversion stages reduce the overall system efficiency.

This paper discusses a topology based on CHB-ISOP configuration, which addresses the limitations mentioned above. The proposed topology is a two-stage solution consisting of AC-DC and isolated DC-DC conversion stages, modified to generate multiple ports which are capable of processing different load powers. This is achieved by incorporating a multi-winding high-frequency Inter-Module Transformer (IMT) at the low-voltage side of the proposed converter. Also, there is no further semiconductor addition or increase in power processed by each semiconductor module compared to the existing ISOP single port structure, or the configuration proposed in [7]. The added IMT also does not require medium voltage insulation as it is located on the low voltage side, unlike in [7]. The topology is also capable of handling bidirectional power flow between DC ports and the MVAC grid. Converter operation and modulation are discussed in the second section, and the simulation results are given in the third section. The fourth section provides the experimental results for a scale down prototype, with the fifth section concluding the paper.

II. Analysis of Proposed Converter

A. Topology description

The topology of the proposed converter is shown in Fig 4. The MVAC is connected through a multi-level cascaded H-bridge (CHB) configuration. Each phase consists of n H-bridges. n is decided by the blocking voltage of CHB devices and the peak of the line to neutral MVAC voltage. CHB is modulated with well known phase-shifted modulation strategy that results in power factor corrected balanced three-phase currents drawn from the MVAC port [8]. There are m load ports. In practical scenario, m¡n. Here we assume n is an integral multiple of m. Each port is connected to r H-bridges of the CHB in each phase. So, m*r=n. Three H bridges from three-phases are combined using a 4-winding high frequency transformer. The fourth winding is connected to an H-bridge interfacing a load port. These 4-winding transformers are termed as main transformer. So, for each LVDC load port there are r 4-winding/main transformers. Each H-bridge interfacing m LVDC load ports are connected to a m-winding transformer. This transformer is called inter-module-transformer.

B. Modulation of the proposed converter

Here modulation refers to the switching strategy for all the H-bridges except the ones in CHB. For simplicity let us assume that there is no power loss in the converter and magnetizing inductance of the transformer is infinity. All H-bridges are modulated with a square wave of a given switching frequency (f_s). All 3r H-bridges connected to a particular LVDC load port j are identically modulated with a phase shift of δ_{jj} with respect to the square-wave generated by the H-bridge connected to port j. Let us assume L_p be the series inductance connected to each of the H-bridge (there are a total of 3n of them) that interfaces the floating DCs of the CHB's and the winding of the main transformers. Let L_s be the series inductance connected between the H-bridge interfacing a LVDC load port and the main transformer. L_s is reflected to the primary of main transformer with a turns ratio of 1:1:1:h as $L'_s = L_s/h^2$.

Power transferred for a dual active bridge (DAB) with phase shift δ, Fig. 5 is given in (1). Similarly for the main transformer in Fig. 6, the relation between power and phase shift for the j^{th} module through main transformer is given in (2). L_{sj} is the equivalent inductance seen from primary to secondary in j^{th} module for the star equivalent shown in Fig. 6 which is $L_{sj} = L'_s + L_p/3$.

$$P = \frac{V_1 V_2}{8 f_s L}\delta(2 - |\delta|) \tag{1}$$

$$P_c = \frac{V_{dc} V_j}{8 h f_s L_{sj}}\delta_{jj}(2 - |\delta_{jj}|) \tag{2}$$

$$P_{ij} = \frac{V_i V_j}{8 f_s L_{ij}}\delta_{ij}(2 - |\delta_{ij}|) \tag{3}$$

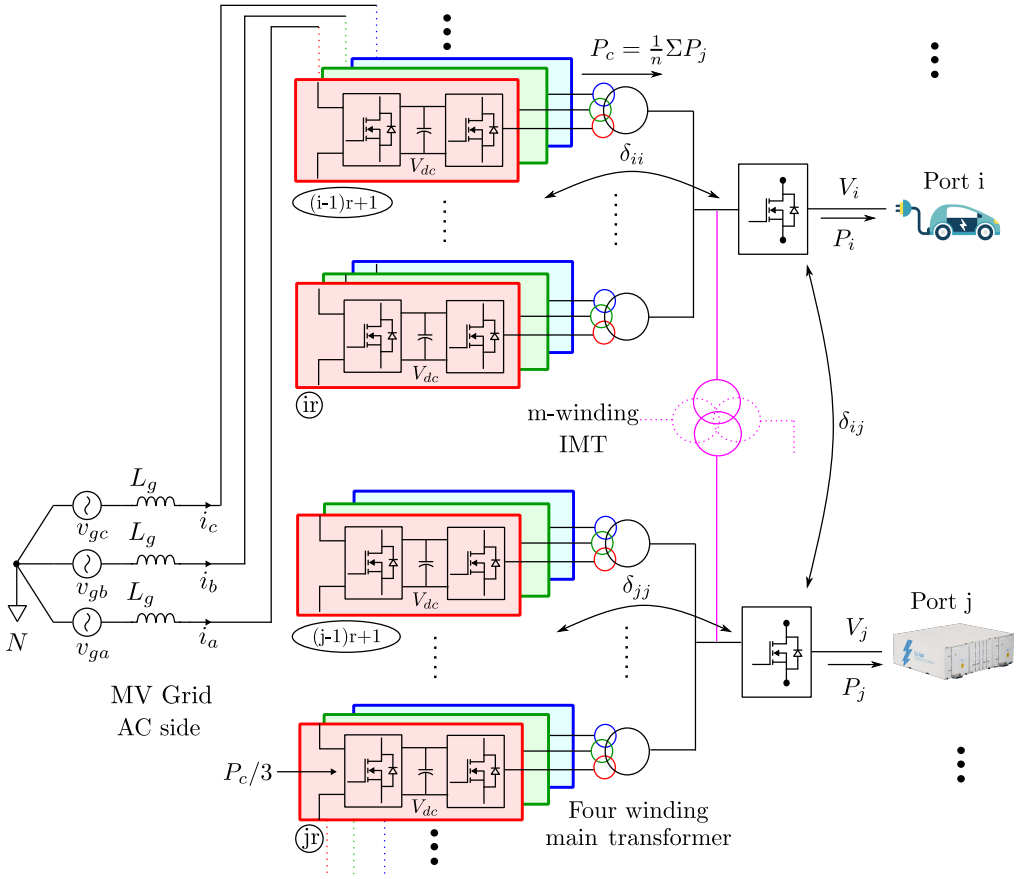

Fig. 4. Proposed Medium Voltage AC to isolated multi-port LVDC topology with inter module transformer (IMT)

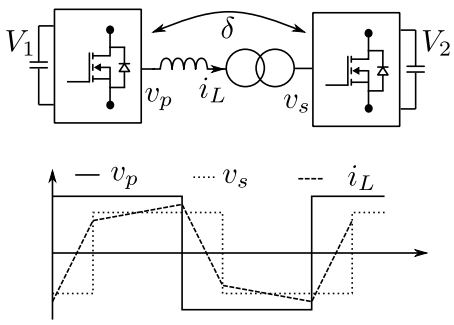

Fig. 5. Power flow in Dual active bridge converter (1) with SPS modulation.

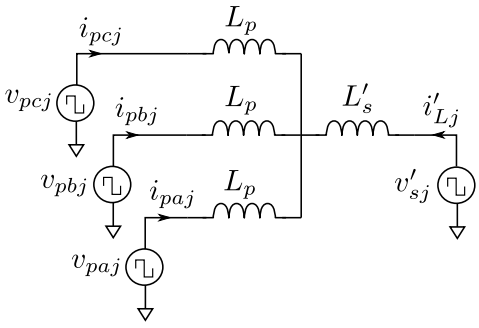

Fig. 6. Power flow in four winding main transformer of j^{th} module (2)

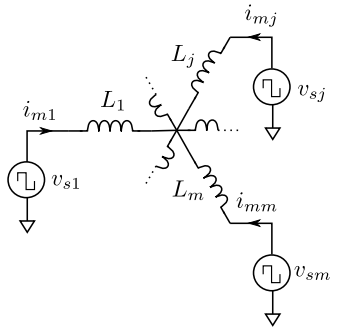

Fig. 7. Power flow in the multi-winding IMT (3)

The phase shift between different bridges on the low voltage side connected to different ports corresponds to the IMT power transfer given in (3). This is shown in Fig. 7 assuming its turns is 1:1 ... :1. V_i and V_j are DC bus voltages of port i and j respectively. δ_{ij} is the phase shift between i^{th} bridge and j^{th} bridge at low voltage side. L_{ij} is the equivalent inductance seen between ports i and j of the IMT. The relation between L_{ij} and equivalent star combination shown in Fig. 7 is as given in (4).

$$L_{ij} = L_i L_j \left(\frac{1}{L_1} + \frac{1}{L_2} + ... + \frac{1}{L_n} \right) \tag{4}$$

III. Simulation Results

Simulations are carried out in the software tool PLECS for the operating condition listed in Table. I with two load ports connected to three-phase AC system (m=2, r=1). There are two load ports, each drawing 25 kW and 10 kW from the three-phase medium voltage grid. A balanced three-phase current of $6.72A = (25kW + 10kW)/(\sqrt{3} * 3kV)$ is drawn from the grid for a total load of 35 kW as given in Fig. 10. The two LVDC load ports are loaded differently, demonstrating the proposed converter's capability to handle the load imbalance.

TABLE I
MEDIUM VOLTAGE AC TO TWO PORT LOW VOLTAGE DC SIMULATION PARAMETERS ($r = 1$)

MVAC L-L[V]	CHB f_s [kHz]	DAB f_s [kHz]	LVDC-1 [V]	LVDC-2 [V]	P_1 [kW]	P_2 [kW]	m	L_p [μH]	L_j [μH]	V_{dc} [V]	Turns ratio (main Tr.)	Turns ratio (IMT)
3000	10	20	800	800	25	10	2	500	100	1300	1:1:1:1	1:1

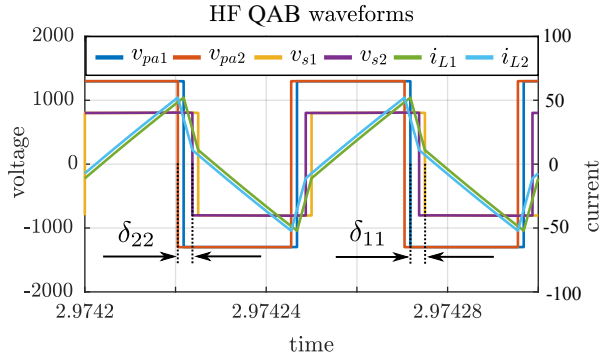

Fig. 8. Simulation waveform for module 1 and 2 in a-phase main transformer.

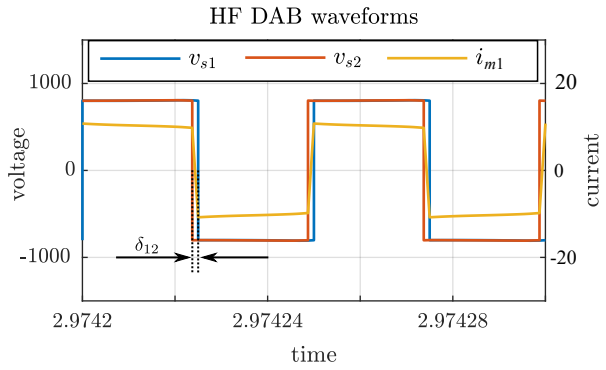

Fig. 9. Low voltage side High Frequency IMT waveform in module 1 and 2.

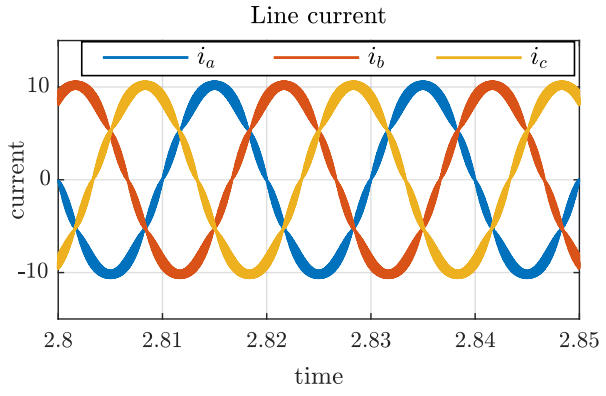

Fig. 10. Balanced three phase line currents at MVAC side

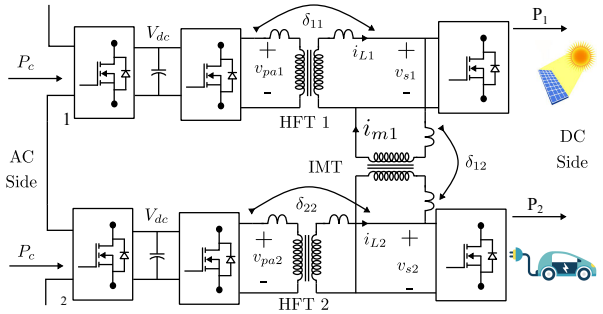

Fig. 11. Schematic of single phase two port structure to demonstrate the proposed configuration with generation in one port and load in other.

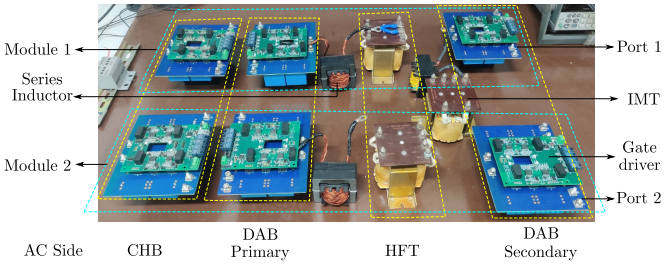

Fig. 12. Single phase two port experimental setup for the specification given in Table. II

The CHB DC bus voltages (V_{dc}) are maintained at 1300V as shown in Fig. 9 (v_{pa1} and v_{pa2}). Fig. 8 indicates both the modules transmitting the same power of $17.5kW$ from the CHB DC bus to the low voltage side. Hence δ_{11} and δ_{22} are dependent on the total load power of all $m(2)$ ports. From (2) the phase shift between the primary and secondary bridge of first module $\delta_{11} = 0.257$ and second module $\delta_{22} = 0.257$ are same in order to transmit 17.5 kW each from CHB DC bus to LVDC side. From (3) the IMT is modulated to have a phase shift between first and second module $\delta_{12} = -0.103$, as given in Fig. 9. 7.5kW is transmitted from module 2 to module 1 with this phase shift.

IV. EXPERIMENTAL RESULTS

Though the simulation studies are carried out for the specifications shown in Table. I, the experiments are carried out at lower power and voltage levels for a single phase two-port structure as shown in Fig. 11. The operating parameters for the experimentation are given in Table. II. The bidirectional power flow capability of the converter is demonstrated in this experiment. LVDC port 1 generating 500W (P_1), is emulated as a source and LVDC port 2, loaded at 125W (P_2), is emulated as a load. The excess power of 375W is transferred

TABLE II
SINGLE PHASE PARAMETERS FOR EXPERIMENT AT LOWER VOLTAGE AND POWER LEVEL SHOWN IN FIG. 12

AC L-N[V]	CHB f_s [kHz]	DAB f_s [kHz]	LVDC-1 [V]	LVDC-2 [V]	P_1 [W]	P_2 [W]	m	L_{pk} [μH]	L_j [μH]	V_{dc} [V]	Turns ratio (main Tr.)	Turns ratio (IMT)
175	10	50	80	80	-500	125	2	55	15	130	1.5:1	1:1

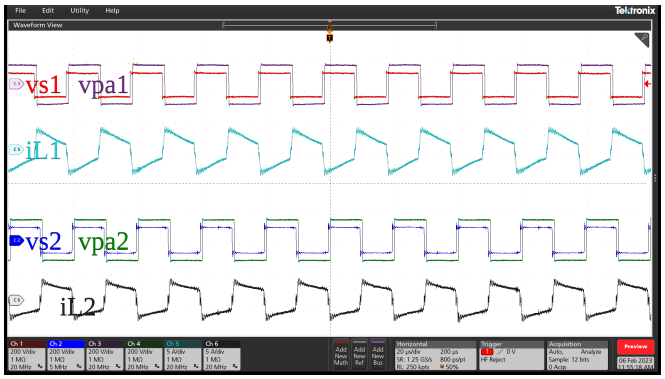

Fig. 13. a-phase primary and secondary DAB waveform for module 1 and 2

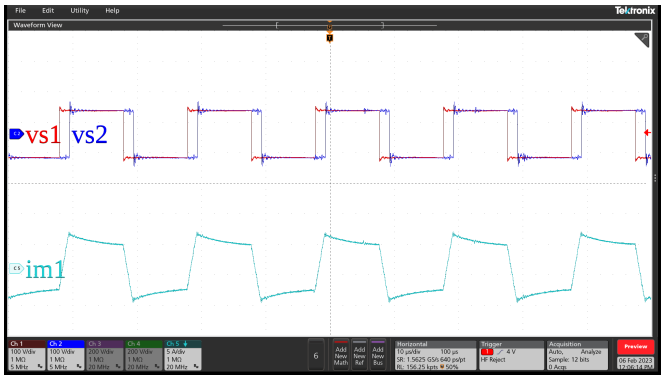

Fig. 14. Module 1 and 2 high frequency DAB waveform at LV side in IMT

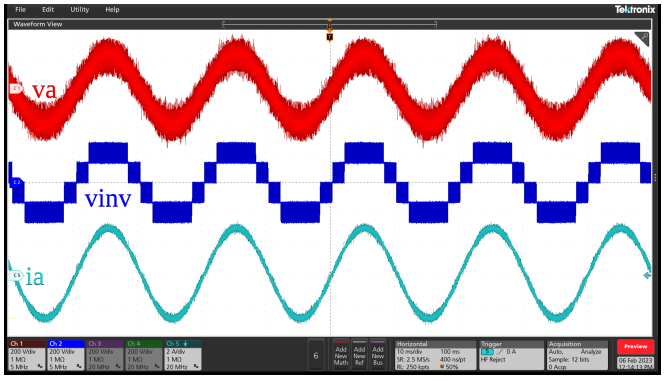

Fig. 15. a phase grid voltage, inverter voltage and current waveform

to the grid with as per (2) and (3). SiC MOSFETs from Genesic (G3R30MT12K) are used to realize the H-bridges in the converter, which are driven by gate driver ADuM4135 from Analog Devices. The CHB module is switched at 10 kHz, and the DAB stage is switched at 50 kHz. While HFTs with a turns ratio of 1.5:1 are used as HFT1 and HFT2, another HFT with a turns ratio of 1:1 is used to emulate the IMT transformer. The photograph of the experimental setup is shown in Fig. 12, where each stage is demarcated. A 1mH inductor is used as a grid-side filter to filter the grid-side AC current.

Fig. 13 shows the high-frequency waveforms with both modules' primary and secondary voltage in a-phase. It can be seen from Fig. 13 that both the modules have the same phase shift ($\delta_{11} = -0.163$ and $\delta_{22} = -0.163$) to transfer the same amount of power from AC to DC ports. The phase shift between the modules ($\delta_{12} = 0.18$) is utilized to transfer the power difference due to load mismatch through IMT, which is highlighted in Fig. 14.

V. CONCLUSION

This paper proposes a novel two-stage MVAC to multiple port LVDC converter with high-frequency isolation. Multiple isolated LVDC ports with different power requirements are catered to without increasing the power rating of semiconductors by adding an additional multi-winding HFT (IMT). The proposed IMT acts as an interface between different load side modules preventing the power mismatch between CHB modules. Since the proposed IMT is situated at the low voltage side, it does not require medium voltage isolation. A modulation strategy for this converter is also proposed to handle different power requirements at different ports in both directions. The capability of the converter to handle independent powers in different ports is demonstrated in this paper with simulation studies and experimental validation.

REFERENCES

[1] "Electric vehicle conductive charging system - Part 23: DC electric vehicle charging station," International Electrotechnical Commission, Geneva, CH, Standard, Mar. 2014.

[2] F. Wang, G. Wang, A. Huang, W. Yu, and X. Ni, "Design and operation of a 3.6kv high performance solid state transformer based on 13kv sic mosfet and jbs diode," in *2014 IEEE Energy Conversion Congress and Exposition (ECCE)*, 2014, pp. 4553–4560.

[3] Y. Yu, G. Konstantinou, B. Hredzak, and V. G. Agelidis, "Power balance optimization of cascaded h-bridge multilevel converters for large-scale photovoltaic integration," *IEEE Transactions on Power Electronics*, vol. 31, no. 2, pp. 1108–1120, 2016.

[4] C. Liu, C. Liu, G. Cai, H. Ying, Z. Zhang, R. Shan, Z. Pei, and X. Song, "An isolated modular multilevel converter (i-m2c) topology based on high-frequency link (hfl) concept," *IEEE Transactions on Power Electronics*, vol. 35, no. 2, pp. 1576–1588, 2020.

[5] H. Saad, X. Guillaud, J. Mahseredjian, S. Dennetière, and S. Nguefeu, "Mmc capacitor voltage decoupling and balancing controls," *IEEE Transactions on Power Delivery*, vol. 30, no. 2, pp. 704–712, 2015.
[6] J. L. A. Maitra, S. Rajagopalan, M. DuVall, and M. McGranaghan, "Medium voltage stand alone dc fast charger," May 30 2013, uS Patent 13/479,389. [Online]. Available: http://www.google.it/patents/US4741207
[7] Y.-S. L.-J. Chang, "Power converting system and control method," Mar. 1 2012, uS Patent US13/831,278.
[8] Y. Ko, M. Andresen, G. Buticchi, and M. Liserre, "Power routing for cascaded h-bridge converters," *IEEE Transactions on Power Electronics*, vol. 32, no. 12, pp. 9435–9446, 2017.